ISSN 2079-1704. Хімія, фізика та технологія поверхні. 2023. Т. 14. № 2. С. 237-248

UDC 66.081.6-278+66.081.62 doi: 10.15407/hftp14.02.237

**K.O. Kudelko [1], L.M. Rozhdestvenska [1], L.M. Ponomarova [2], V.M. Ogenko [1]**

# ANODIC ALUMINUM OXIDE-MEMBRANE PREPARED IN ELECTROLYTE "OXALIC ACID – MATTER WITH CARBON NANODOTS"

*[1] V.I. Vernadskyy Institute of General and Inorganic Chemistry of National Academy of Sciences of Ukraine*
*34/34 Palladin pr., Kyiv, 03141, Ukraine, E-mail: kathykudelko@gmail.com*
*[2] Faculty of Technical Systems and Energy Efficient Technologies, Sumy State University*
*2 Rimsky-Korsakov Str., Sumy, 40007, Ukraine, E-mail: ponomarouva@gmail.com*

*Anodic porous alumina has been studied and used as nanoscale structure, coating, template in different applications. The porous anodic alumina oxide could be described as numerous hexagonal cells and looks like cellular structure. In this work we report about results of study anodizing of aluminum with usage of electrolyte: "oxalic acid electrolyte-matter with carbon nanodots". It was received anodic aluminum oxide-membrane with aluminum supporting; calcination was used as post treatment. The aluminum substrate allows one to fix the membrane in the cells. Methods: processes of anodizing was provided in 0.3M oxalic acid with addition of colloid system of carbon nanodots, temperature of process was controlled at range of 10 degree Celsius, aluminum foil (anode) and platinum plate (cathode) were used; thickness of aluminum foil was 0.1 μm; morphology and structure of anodic aluminum oxide-membrane were determined with usage of electron scanning microscope; the contact angle between the surface of anodic aluminum oxide-membrane and deionized water was measured with "drop" methodology. Calcium content was monitored with a conductometer. The content of proteins was determined with photometry (micro Lowry's method). It was found that contact angle of the surface of anodic aluminum oxide-membrane obtained in electrolyte "oxalic acid-matter with carbon nanodots" and deionized water is 38 degrees. Adding colloidal system of carbon nanodots to the acid electrolyte acts as a hydrophilizer, changes the size of the porous surface: as a result, it is possible to control the porosity of the films. Calcination of anodic aluminum oxide-membrane at 500 degree Celsius lead to expansion and thinning of pore walls. Anodic aluminum oxide-membrane was tested for dialysis process for milk whey separation. The membrane obtained in electrolyte: "oxalic acid-matter with carbon nanodots" showed a greater degree of rejection of protein particles in comparison with a similar membrane obtained in electrolyte of oxalic acid. The advantage of using carbon nanodots in acid electrolyte is the simplicity and environmental friendliness of the synthesis. The approach, which involves the addition of a colloidal system with carbon nanomaterial, allows one to avoid using a strongly acidic electrolyte for obtaining membranes with smaller pores. One of the ways for using of anodic oxide aluminum-membrane is the dialysis of biological fluids, for example, milk whey.*

***Keywords**: anodized aluminum oxide, carbon nanodots, oxalic acid, colloid system, electrochemical synthesis, dialysis*

## INTRODUCTION

Freshly precipitated or aged hydrated alumina oxide (HAO) is widely used as a flame retardant filler [1], precursor to Al compounds (aluminum chloride [2], zeolites [3], activated alumina [4] *etc*.) and also in pharmaceutical industry [5, 6], particularly for the preparation of drugs against COVID-19 [5] and Ebola fever [6]. Other field of application of this material is adsorbents for water treatment [7–9] particularly as a constituent of double oxides [10–12] As opposed to widespread phosphates of multivalent metals, which possess cation exchange properties [13–15], HAO demonstrates also anion exchange capability in acidic media, whereas it adsorbs cations in alkaline media [16]. HAO is also applied to modifying membranes in order to provide the improvement of their separation or transport capability and hydrophilicity [17–20] similarly to hydrated zirconium dioxide [21–24].

Among amorphous oxide materials, anodic aluminum oxide (AAO) occupies special position due to regular porous structure [25–27]. AAO is synthesized to protect the aluminum surface from corrosion - the first patent was obtained in Great Britain in 1923. On the other hand, AAO-film provides a porous textures of the metal surface, which is necessary for applying paint and varnish. It is possible to

obtain mechanically stable membranes with regular and through pores [28–32], particularly after calcination. The membranes are used for the separation of biogenic particles of different size [33] and even particles with similar molecular mass [34], for the purification of biological liquids from urea, creatinine, vancomycin and inulin [35], for sensors [36–38], catalyst carriers [39], as separators for lithium-ion batteries [40, 41]. AAO-membranes containing adsorbed metal cations are capable to adsorb proteins [42]. The membranes are used as some matrices for growing nanostructures such as carbon [43, 44], polyaniline [45], titanium [46] nanotubes. Thus, AAO has a wide field of practical application.

As noted in the review [47], the smallest pores are formed in the solution of strong acid ($H_2SO_4$, $H_2SeO_4$). Regarding weaker acids, such as $H_3PO_4$, $C_2H_2O_4$, it is possible to obtain larger pores. This is due to proportionality of pore diameter to the voltage, at which anodization was performed. Decrease of the solution resistance reduces the voltage; as a result, smaller pores are formed. However, this approach is undesirable from the point of view of safety and environmental protection. Other way is screening the anode with inert nanoparticles reducing its working surface area. Earlier it has been shown that the additions of graphene oxide (GO) to the solution of oxalic acid results in a decrease of AAO pore size [48]. This is evidently due to adsorption of GO nanosheets on the aluminum surface – this is typical behavior for GO and metals [49–53]: the nanosheets are adsorbed on the electrode surface through the π–π-stacking interaction with graphene. Moreover, GO is included into AAO during Al anodization [48]: this is similarly to the composite formation over precipitation of hydrated metal oxide simultaneously with GO [54–56]. The GO addition evidently increases AAO hydrophilicity, since this nanomaterial is used for hydrophilization of polymer membranes to improve their resistance against fouling with organic substances [57–59]. The goal of work is to examine other carbon nanomaterial to evaluate its effect on porous structure of AAO. In this case, 0-dimentional carbon nanodots (CNDs) were chosen instead of 2-dimentional GO. The size of these nanoparticles is smaller comparing with GO nanosheets, but the chemical composition of the surface is similar. Thus, it is possible also to expect their effect on the porous structure of AAO.

## EXPERIMENTAL

Carbon nanodots were obtained according to the method [60]. Briefly: citric acid (1.05 g) was dissolved in 10 $cm^3$ of deionized water, then ethylenediamine (0.33 $cm^3$) was added. The solution was inserted into reactor which was plugged up and heated at 200 degrees Celsius during 5 h. The size of CNDs obtained by this manner was 8–12 nm, as noted in [60]. This procedure was repeated several times to obtain a considerable volume of colloidal system of carbon nanoparticles. The amount of solid in aqueous medium was determined with gravimetric technique. As found, the amount of CNDs in colloidal system was 110 g $dm^{-3}$.

The aliquot ($cm^3$) of the CNDs solution was inserted to a 0.3 M $H_2C_2O_4$ solution, the resulting content of carbon constituent was 0.0015 g·$dm^{-3}$. Before the electrochemical experiment, the solution was activated with ultrasound at 30 kHz during 10 min using an ultrasonic bath (Bandelin, Hungary).

Technically pure aluminum plate, a thickness of which was 0.1 mm, was used as an anode. The material contained (at. %): Al – 99.97 %, Fe – 0.01 %, Si – 0.01 %, Cu – 0.01 %. The method for the pretreatment of the aluminum plate is described in detail earlier [48]. The procedure involved calcination, ultrasonic treatment, washing with ethanol and coating of one side with a mask of photoresist. 37 rounds were present on photoresist mask. The diameter of one round was 3 mm. From the mask side, the plate was polished subsequently with solutions $CuCl_2$ and HCl, and rinsed out with deionized water.

The description of the experimental setup is given in [48]. Briefly: the stack contained electrochemical parallel-plates reactor, where the electrodes were vertical. The reactor consisted of 2 compartments, the first chamber contained electrodes and electrolyte, the second one remained empty. The compartments were separated with Al plate. The electrolyte was cooled down to 10 °C during pumping through the reactor. The side of the anode, which was coated with perforated mask. The cell voltage was 40 V. In order to remove the additions of other metals, the impulse of 100 V was given (2 s) at the start of anodizing.

Electrochemical oxidation of aluminum was carried out in two stages [61], when the solution of oxalic acid without CNDs was used. The duration of the first stage was 2 h, then the AAO-layer was removed with a mixture of $H_2CrO_4$ and 6% $H_3PO_4$ similarly to [48]. Further the second stage was carried out in the same condition.

When the electrolyte containing both oxalic acid and CNDs was used, one-stage process was performed. The residual aluminum was removed with a $CuCl_2$ solution in concentrated HCl, then the plate was treated with a $H_3PO_4$ solution to remove the AAO-layer with non-regular pores.

Morphology and chemical composition of AAO were performed using a Tescan Mira 3LMU scanning electron microscope supplied with an In Beam detector (TESCAN, Czech Republic). Two independent variants of sample's coating (carbon and gold) were used in research, a Gatan pecs 682 preparation device (Gatan, Inc., USA) was applied to this purpose. The time to provide vacuum conditions was 15 min. Focusing and astigmatism compensation were used to obtain clear images.

The AAO membrane obtained in a presence of carbon additions was tested for dialysis of biological liquids. Dialysis of milk whey (produced by Pyryatin Syrzavod LTD) was performed through the AAO membrane using the cell described above. The biological liquid filled the first compartment, deionized water circulated through the second chamber. Milk whey contained 7 g $dm^{-3}$ of salts. The control of salt content in the solution, which was formed as a result of diffusion, was carried out with a conductometer HI 9932 (Hanna Instruments, Germany). The content of proteins was determined with photometric method [62].

## RESULTS AND DISSCUSION

Regarding carbon addition to the oxalic electrolyte, the advantage of CNDs over GO is a simplicity and ecological purity of synthesis. Moreover, not only chemical reagents [60] but also natural raw material like polysaccharides [63] can be used for the synthesis procedure. As found early with a high-resolution TEM observation, the shape of CNDs was close to round, the size of them was 8–12 nm [60]. Since the carbon constituent is nanosized, it gives colloidal system, which demonstrates typical Tyndall cone (Fig. 1 *a*). The color of the solution is orange. Blue luminescent glow is visible in the darkness, when the vessel containing the colloidal system is under UV lamp (Fig. 1 *b*). As shown below, the CNDs additions to electrolyte affects porous structure of AAO.

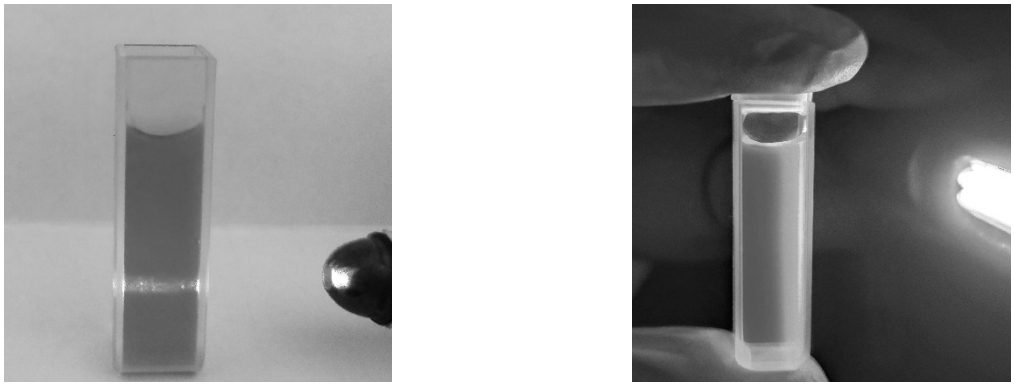

*a* *b*

**Fig. 1.** Tyndall cone through the colloidal system of CNDs (*a*) and its luminescence under UV-irradiation (*b*)

When there is no carbon addition in the oxalic electrolyte, the diameter of the AAO-pores ($d$) is proportional to the cell voltage ($U$) [64]:

$$d = kU\sqrt{\varepsilon}, \quad (1)$$

where $\varepsilon$ is the porosity, $k$ is the empirical constant. Since $U = E_c + E_a + IR$ (here $E_c$ and $E_a$ are the potentials of cathode and anode respectively, $I$ is the current, $R$ is the value that includes the resistances of electrolyte and AAO film), it is possible to write:

$$d = k(|E_c| + E_a + iSR)\sqrt{\varepsilon}, \quad (2)$$

where $i$ is the current density, $S$ is the effective surface area of the anode. Adsorbed CNDs partially isolate the anode surface; it means a decrease of the $S$ value. As a result, smaller pores should be formed.

Indeed, the effect of CNDs additions on current is seen in Fig. 2. The CNDs additions decrease current in ~ 2 times. Since no change of the electric conductivity of oxalic electrolyte was found after CNDs insertion, reducing current is due to screening of the electrode surface.

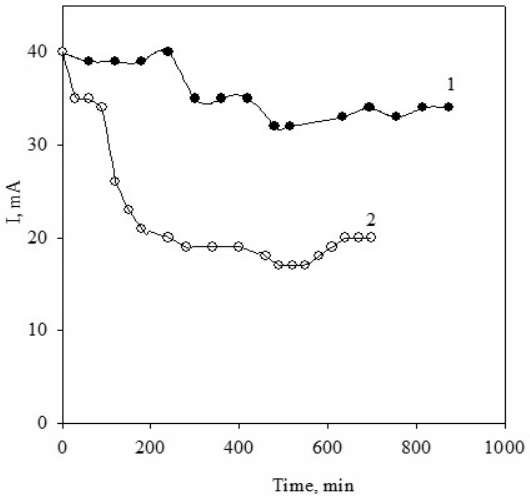


**Fig. 2.** Current as a function of time of aluminum anodizing (second stage). Electrolyte was without (*1*) and with CNDs (*2*)

Fig. 3 illustrates pore structure of AAO obtained without and with carbon additions, the samples were observed before the removal of bottom side of AAO (i.e. residual aluminum) and after its removal (i.e. after the pore opening). Regarding the sample synthesized in the absence of CNDs cellular structure of pores are seen, the length of the hexagon side is about 23 nm. The thickness of pore walls is up to 30 nm. The pores diameter is within the diapason of 50–100 nm; the largest pores dominate. From the bottom side, the convex in homogeneities are seen, their shape is irregular but close to spherical. Their diameter is 75–100 nm. The pores are through and cylindrical, the outer diameter of empty cylinders is 140–160 nm, the inner diameter corresponds to the $d$ value of holes.

In the case of AAO obtained in the presence of CNDs, it surface is more irregular comparing with the sample, which was synthesized without carbon additions. Though the length of pore walls are also ≈ 23 nm, their thickness is larger (up to 50 nm), the hole diameter is 20–40 nm. The outer diameter of cylindrical pores is up to 85 nm, the convex inhomogeneities are also seen in the bottom side of AAO.

Thus, the CNDs additions provide formation smaller pores with thicker walls evidently due to the screening the electrode surface with nanoparticles. According to the formula (2), decrease of the effective area of the electrode reduces the current, when anodizing occurs under potentiostatic conditions. Other way to decrease pore size is to reduce the cell voltage. However, in this case the formation of the AAO layer is more long-time.

The effect of carbon additions can be explained also from the point of view of the mechanisms of AAO growth. First of all, the nanosheets of the materials of GO type are adsorbed on the surface of hydrated oxides [65, 66]. Let us consider the influence of non-conducting nanosheets on the AAO-film growth taking different theories into consideration. The theory of Bogoyavlensky is considered AAO as colloid formations [67]. According to this theory, the anodic oxide is the gel of metal oxide. First the embryos of future micelles are formed on the active centers of the anode. The embryos grow and turn into polyions: they are fibrous rod-shaped micelles that form skeleton of oxide gel. Adsorption of anions and water, which is carried

out due to their transport in intermicellar pores, provides the negative charge of the micelles. Similarly, to GO-, the CNDs-surface is practically unchanged in acidic media, this provide adsorption of nanodots on the micelles. Since CNDs tend to aggregation, they can perform a function of a cross-linking agent for micelles, which are elongated along the direction of electric field.

Both the negative charge of micelles [67] and migration of $O^{2-}$ ions through the film being formed towards positively charged anode [68] provide AAO adhesion to aluminum. Screening of AAO-micelles with CNDs depresses anion migration, this results in a decrease of current. Moreover, adsorbed carbon addition, which possesses no electron conductivity, increases the resistance of the AAO-film. As a result, the current decreases (see Fig. 2). Screening of the electrode with AAO promotes adsorption of CNDs.

Hydrophilic properties of ceramic membrane were tested with deionized water; the drop was spread over a surface.

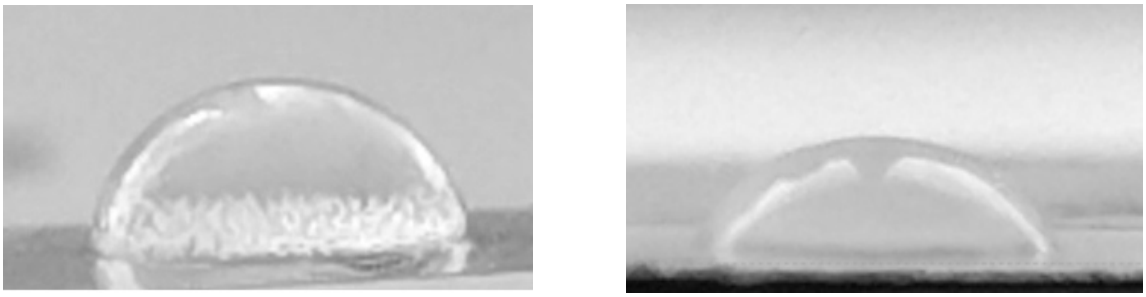

*a* *b*

**Fig. 3.** Contact angle: AAO-membrane (*a*), AAO-membrane with CND (*b*)

According to the mechanical model, the volume of HAO (i.e. AAO) being formed is 2 times larger comparing with metal aluminum [69]. Pores are a result of volumetric expansion of aluminum oxide. Indeed, the density of aluminum is 2.7 $g \cdot cm^{-3}$, the value for crystalline $Al_2O_3$ is 3.95 $g \cdot cm^{-3}$. However, the density of tightly packed sheets of graphene (2.27 $g \cdot cm^{-3}$) is close to that for graphite. It means, adsorption of carbon additions decreases the volume of AAO so depressing mechanical stress.

The assumption of CNDs adsorption on AAO is confirmed by the data of chemical analysis. Fig. 5 illustrates typical electron spectrum obtained for AAO, the data of chemical composition are given in Table (the content of oxygen, as determined using the SEM-equipment, corresponds to the summary content of oxygen and hydrogen).

**Table.** Chemical composition of AAO-membrane (all lines are K-series, the analysis was made for the samples with opened pores, carbon layer was sprayed)

| Element | Content, % | | | |
|---|---|---|---|---|
| | mass | | atomic | |
| | without CNDs | with CNDs | without CNDs | with CNDs |
| O | 21.55 | 23.49 | 22.61 | 29.02 |
| Al | 37.72 | 55.79 | 23.47 | 40.86 |
| C | 33.90 | 17.50 | 47.38 | 28.79 |
| Cu | 1.48 | 2.02 | 0.39 | 0.63 |
| S | 0.41 | 0.53 | 0.21 | 0.33 |
| N | 4.95 | 0.57 | 5.93 | 0.01 |
| Total | 100 | 100 | 100 | 100 |

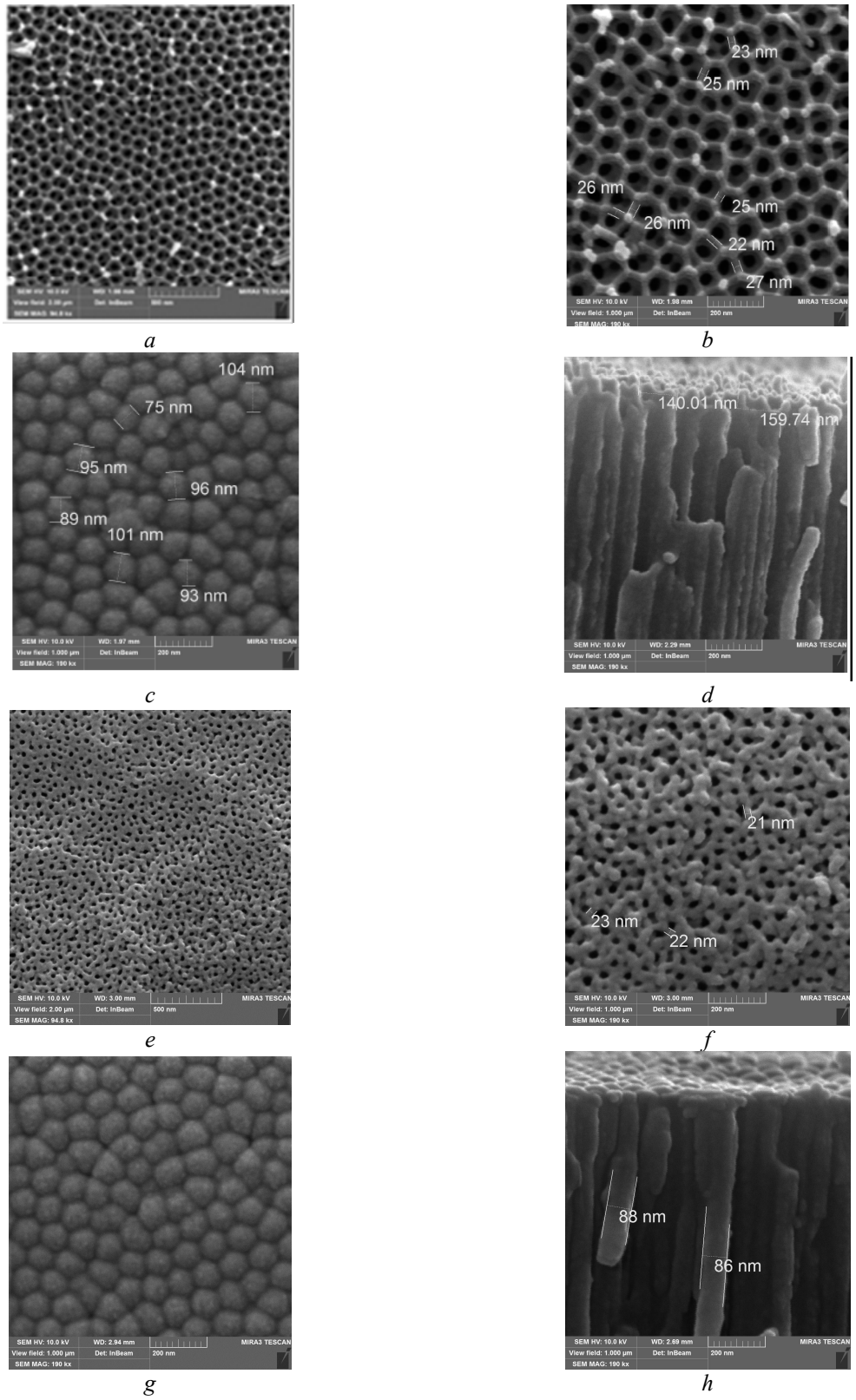


**Fig. 4.** SEM-images of AAO-membranes synthesized without (*a-d*) and with (*e-h*) CNDs. The images were obtained after carbon (*a*, *e*) and gold (*b-d*, *f-h*) coating. The photo illustrates the top (*a*, *b*, *e*, *f*), bottom (*c*, *g*) sides of the AAO-film and its cross-section. The observation was carried out before (*a*, *b*, *d*, *e*, *f*, *h*) and after (*c*, *g*) pore opening

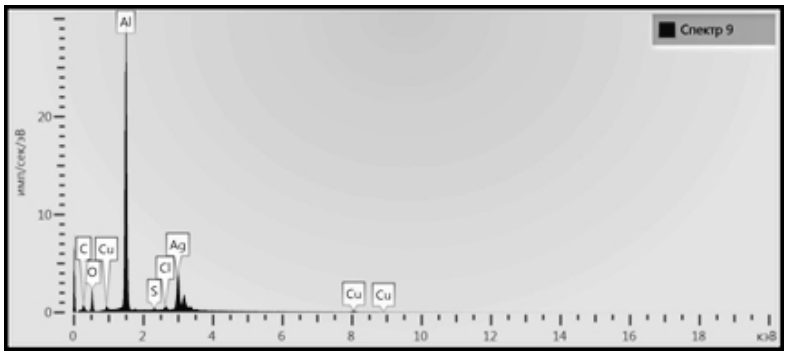


**Fig. 5.** Electron spectrum of AAO obtained in a presence of CNDs. An ultrathin carbon layer was coated

As shown from the Table, AAO-membrane contained sulfur and nitrogen, which were initially in the aluminum plate. The content of copper is due to adsorption of $[Cu(H_2O)Cl_4]^{2-}$-complexes on AAO (normally adsorption of anions on metal oxides is realized in acidic and neutral media [70]), adsorption of CNDs depress anion exchange capability of the metal oxide: smaller copper content was found for the sample obtained in a presence of carbon addition. It is the same for the adsorption of oxalate ions and complexes of aluminum oxalate:

$$2(=A1-OH)+2H^{+}+C_2O_4^{2-}\rightarrow(=A1-OH_2)_2(C_2O_4), \quad (3)$$

$$3(=A1-OH)+3H^{+}+[A1(C_2O_4)_3]^{3-}\rightarrow \rightarrow(=A1-OH_2)_3[A1(C_2O_4)_3]. \quad (4)$$

As a result, smaller ratio of Al:O for the sample, which was obtained in a presence of CNDs, is due to the depression of adsorption of oxygen-containing complexes. The C-content is not indicative, since the sample were coated namely with carbon film.

When the samples were coated with a golden film, the average carbon content was 22 (AAO obtained without carbon addition) and 32 % (AAO-film synthesized in a presence of CNDs). This indicates inclusions of not only carbon of oxalate anions, but also CNDs.

The membrane material containing AAO inclusion is metal substrate illustrated on Fig. 6. The substrate allows us to fix the pore membrane in the cells.

At last, experiment with calcination of AAO-material at 500 °C shown the result of pore widening and pore walls thinning (Fig. 7, compare with Fig. 4 *a*, *e*). Regarding the sample containing CNDs, the pore size increased up to ≈ 50 nm. The surface roughness is saved after thermal treatment. In the case of AAO that includes no carbon addition, the pore diameter reaches ~ 70–100 nm. The pore widening is due to water losses, carbon burnout and crystallization of HAO. Besides pore expansion, the disadvantage of thermal treatment is separation of the AAO-membrane from the metal substrate. In order to save the fixing membrane in the substrate, other approaches have to be used.

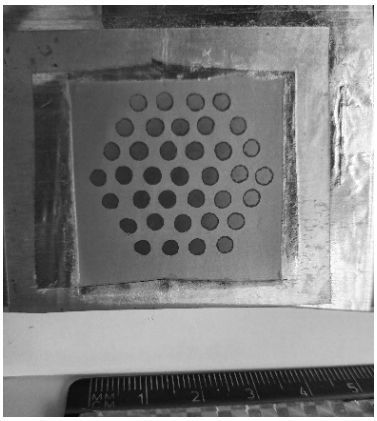

**Fig. 6.** AAO-membrane in aluminum substrate

The AAO-membrane, which was obtained in a presence of CNDs, was tested in the dialysis process to desalt milky whey (no previous calcination was applied). The salt content from the receiving side of the membrane is given in Fig. 8 as a function of time. The salt flux through the membrane, *N*, was calculated as:

$$N = \frac{dn}{dt}\frac{1}{S}, \quad (5)$$

where *n* is the salt amount, *t* is the time. During the first 500 min, the salt amount from the

receiving side of the membrane was $6\times10^{-4}$ kg. Since the effective area of the membrane was $7.1\times10^{-4}$ m$^2$, the salt flux was estimated as $2.82\times10^{-5}$ kg·m$^{-2}$·s$^{-1}$. About 100 g of salts are removed during 1 h, when $S = 1$ m$^2$. In order to reach 50 % of desalination for 1 dm$^3$ of whey, 3.5 g have to be removed during 1 h, It means, the effective area of the AAO membrane is 350 cm$^{-2}$, if the AAO-"window" is square, its size is 18.7×18.7. Other way is to sorb ions, which are moved through the membrane. This is necessary to maintain a constant salt flux. It is possible to use ion exchange resins for this purpose. Direct whey desalination by means of ion exchange is undesirable, since the pH deviations cause protein aggregation and mixing aggregates with resins. If to keep the salt flux at the initial level, it is possible to continue dialysis time. In this case, the membrane area should be decreased.

It should be stressed that the protein rejection was ~ 99 %. Thus, one way of the AAO-membrane application is desalination of small volumes of biological liquids. At the same time, the membrane obtained in an absence of CNDs shows 50 % of rejection of protein particles.

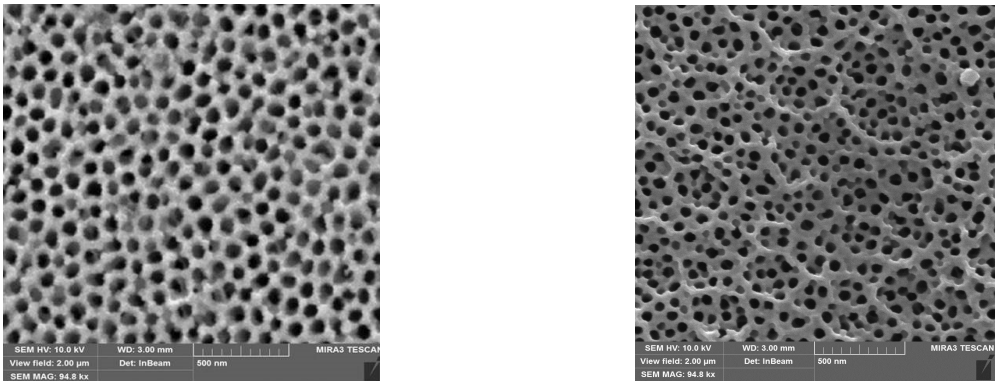


*a* *b*

**Fig. 7.** SEM-images of AAO-membrane synthesized without (*a*) and with (*b*) CNDs followed by calcination

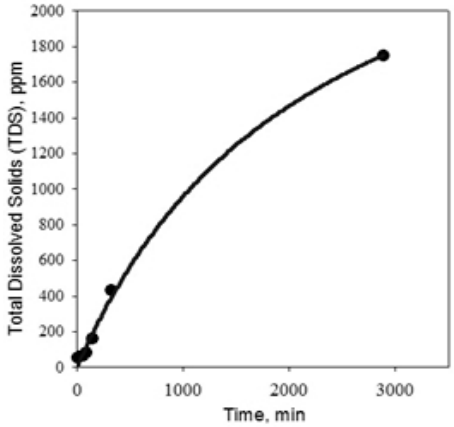


**Fig. 8.** Dialysis desalination of milk whey using AAO-membrane obtained in a presence of CNDs

## CONCLUSIONS

Comparing the data of this work with earlier results [48] allows us to suggest that the usage of both graphene oxide (2-dimensional carbon material) and CNDs (0-dimensional) as additions to weakly acidic electrolyte gives similar results. In other words, mentioned carbon nanomaterials provide formation of smaller pores in AAO. However, the advantage of CNDs is the simplicity and environmental friendliness of synthesis. The approach, which involves the use of carbon nanomaterial, allows us to avoid strongly acidic electrolyte to obtain the

membranes with small pores. This provides ecological friendless of the AAO synthesis.

As shown, one way of application of the obtained AAO membrane is dialysis of biological liquids. The features of these processes is a subject of further investigations. Other directions of practical employment of the membranes, particularly calcined ones, should be also researched.

## Анодна оксидна алюмінієва мембрана, отримана в електроліті «щавлева кислота-матеріал з вуглецевими наноточками»

**К.О. Куделко, Л.М. Рождественська, Л.М. Пономарова, В.М. Огенко**

*Інститут загальної та неорганічної хімії ім. В.І. Вернадського Національної академії наук України*
*пр. Палладіна, 34/34, Київ, 03141, Україна, kathykudelko@gmail.com*
*Факультет технічних систем та енергоефективних технологій, Сумський Державний університет*
*вул. Римського-Корсакова, 2, Суми, 40007, Україна, ponomarouva@gmail.com*

*Анодний оксид алюмінію досліджується та застосовується як нанорозмірні структури, покриття, шаблони та ін. Пористу структуру анодного оксиду алюмінію можна описати як поверхню, що складається з численних гексагональних комірок та характеризується «комірчастою структурою». У роботі викладені результати дослідження анодування алюмінію з використанням електроліту: «щавлева кислота-матеріал з вуглецевими наноточками». Отримано мембрану анодного оксиду на алюмінієвій підкладинці; мембрану додатково прожарювали. Використання субстрату-алюмінію дозволяє закріпити кераміку анодного оксиду алюмінію в отворах. Методи: анодування проводили в 0.3 М щавлевій кислоті з додаванням колоїдної системи вуглецевих наноточок та без них, температури процесів контролювалася на рівні 10 °С, використовували алюмінієву фольгу (анод) та платинову пластину (катод); товщина алюмінієвої фольги 0.1 мкм; морфологію та структуру поверхні анодного оксиду алюмінію визначали за допомогою скануючого електронного мікроскопа; кут змочування між поверхнею анодної оксидної-мембрани та деіонізованою водою вимірювали за допомогою методики «краплі». Вміст кальцію контролювали кондуктометром. Концентрацію білків визначали спектрофотометрично (метод Лоурі). Встановлено, що кут змочування для деіонізованої води у точці дотику з поверхнею анодного оксиду алюмінію отриманого в електроліті «щавлева кислота-матеріал з вуглецевими наноточками» становить 38°. Додавання до кислого електроліту вуглецевих наноточок діє як гідрофілізатор, змінює розмір пористої поверхні: в результаті можливо контролювати пористість плівок. Прожарювання мембрани анодного оксиду алюмінію при 500 °С приводить до розширення пор і стоншення їхніх стінок.*

*Мембрану анодного оксиду алюмінію застосовано для діалізу молочної сироватки. Мембрана, отримана в електроліті «щавлева кислота-матеріал з вуглецевими наноточками», показала більшу ступінь відбиття білкових частинок в порівнянні з аналогічною мембраною, отриманою в електроліті щавлева кислота. Перевагою використання вуглецевих наноточок в електроліті є простота й екологічність синтезу. Підхід, який передбачає додавання колоїдної системи з вуглецевим матеріалом, дозволяє не використовувати сильнокислого електроліту для отримання мембран з порами меншого розміру. Одним із варіантів застосування отриманої анодної оксидної алюмінієвої-мембрани є діаліз біологічних рідин, наприклад, молочної сироватки.*

***Ключові слова**: анодований оксид алюмінію, вуглецеві наноточки, щавлева кислота, колоїдна система, електрохімічний синтез, діаліз*

REFERENCES


1. Hull T.R., Witkowski A., Hollingbery L. Fire retardant action of mineral fillers. *Polym. Degrad. Stab*. 2011. **96**(8): 1462.
2. Patent US 4415412. Vandegrift G.F., Horwitz P., Krumpelt M. Production of anhydrous aluminum chloride composition and process for electrolysis thereof. 1983.
3. Mohamed R.M., Ismail A.A., Kini G., Ibrahim I.A., Koopman B. Synthesis of highly ordered cubic zeolite A and its ion-exchange behavior. *Colloids Surf., A*. 2009. **348**(1–3): 87.
4. Das B.R., Dash B., Tripathy B.C., Bhattacharya I.N., Das S.C. Production of η-alumina from waste aluminium dross. *Miner. Eng*. 2007. **20**(3): 252.
5. Hsieh S.-M., Liu M.-Ch., Chen Y.-H., Lee W.-S., Hwang Sh.-J., Cheng Sh.-H., Ko W.-Ch., Hwang K.-P., Wang N.-Ch., Lee Yu-L., Lin Yi-L., Shih Sh.-Ru, Huang Ch.-G., Liao Ch.-Che, Liang J.-J., Chang Ch.-Sh., Chen Ch., Lien Ch. En, Tai I-Ch., Lin T.-Y. Safety and immunogenicity of CpG 1018 and aluminium hydroxide-adjuvanted SARS-CoV-2 S-2P protein vaccine MVC-COV1901: interim results of a large-scale, double-blind, randomised, placebo-controlled phase 2 trial in Taiwan. *Lancet Respir. Med*. 2021. **9**(12):1396.
6. Fleagle Chisholm C., Jin Kang T., Dong M., Lewis K., Namekar M., Lehrer A.T., Randolph T.W. Thermostable ebola virus vaccine formulations lyophilized in the presence of aluminum hydroxide. *Eur. J. Pharm. Biopharm*. 2019. **136**: 213.
7. Zotov R., Meshcheryakov E., Livanova A., Minakova T., Magaev O., Isupova L., Kurzina I. Influence of the composition, structure, and physical and chemical properties of aluminium-oxide-based sorbents on water adsorption ability. *Materials*. 2018. **11**(1): 132.
8. Danilevich V.V., Isupova L.A., Kagyrmanova A.P., Kharina I.V., Zyuzin D.A., Noskov A.S. Highly effective water adsorbents based on aluminum oxide. *Kinet. Catal*. 2012. **53**(5): 632.
9. Islam M.A., Morton D.W., Johnson B.B., Pramanik B.K., Mainali B., Angove M.J. Metal ion and contaminant sorption onto aluminium oxide-based materials: a review and future research. *J. Environ. Chem. Eng*. 2018. **6**(6): 6853.
10. Mal'tseva T.V., Kudelko E.O., Belyakov V.N. Adsorption of Cu(II), Cd(II), Pb(II), Cr(VI) by double hydroxides on the basis of Al oxide and Zr, Sn, and Ti oxides. *Russ. J. Phys. Chem. A*. 2009. **83**(13): 2336.
11. Mal'tseva, T.V., Yatsenko, T.V., Kudelko, E.O., Belyakov V.N. The effect of introduction of manganese hydroxide and hydrated aluminum oxide on the pore structure and surface charge of Zr(IV), Ti(IV), and Sn(IV) oxyhydrates. *Russ. J. Appl. Chem*. 2011. **84**: 756.
12. Mal'tseva T.V., Pal'chik A.V., Kudelko E.O., Vasilyuk S.L., Kazdobin K.A. Impact of surface properties of hydrated compounds based on $ZrO_2$ on the value of ionic conduction. *J. Water Chem. Technol.* 2015. **37**(1): 18.
13. Dzyazko Y.S., Rozhdestvenska L.M., Palchik A.V. Ion-exchange properties and mobility of $Cu^{2+}$ ions in zirconium hydrophosphate ion exchangers. *Sep. Purif. Technol.* 2005. **45**(2): 141.
14. Pal'chik A.V., Dzyazko Yu.S., Rozhdestvenskaya L.M. Recovery of nickel ions from dilute solutions by electrodialysis combined with ion exchange. *Russ. J. Appl. Chem.* 2005. **75**(3): 414.
15. Wu Y., Chen J., Liu Zh., Nab P., Zhang Zh. Removal of trace radioactive $Cs^+$ by zirconium titanium phosphate: From bench-scale to pilot-scale. *J. Environ. Chem. Eng.* 2022. **10**(4): 108073.
16. Amphlett B. *Inorganic Ion Exchangers*. (New York: Elsevier, 1964).
17. Wang X.-M., Li X.-Y., Shih, K. In situ embedment and growth of anhydrous and hydrated aluminum oxide particles on polyvinylidene fluoride (PVDF) membranes. *J. Memb. Sci.* 2011. **368**(1–2): 134.
18. Saleh T.A., Gupta V.K. Synthesis and characterization of alumina nano-particles polyamide membrane with enhanced flux rejection performance. *Sep. Purif. Technol.* 2012. **89**: 245.
19. Branchi M., Sgambetterra M., Pettiti I., Panero S., Navarra M.A. Functionalized $Al_2O_3$ particles as additives in proton-conducting polymer electrolyte membranes for fuel cell applications. *Int. J. Hydrogen Energy*. 2015. **40**(42): 14757.
20. Yang C.-C., Chiu S.-J., Chien W.-C., Chiu S.-S. Quaternized poly(vinyl alcohol)/alumina composite polymer membranes for alkaline direct methanol fuel cells. *J. Power Sources*. 2010. **195**(8): 2212.
21. Myronchuk V., Zmievskii Yu., Dzyazko Yu., Rozhdestvenska L., Zakharov V. Whey desalination using polymer and inorganic membranes: Operation conditions. *Acta Periodica Technologica*. 2018. **49**: 103.
22. Dzyazko Yu., Rozhdestveskaya L., Zmievskii Yu., Volfkovich Yu., Sosenkin V., Nikolskaya N., Vasilyuk S., Myronchuk V., Belyakov V. Heterogeneous membranes modified with nanoparticles of inorganic ion-exchangers for whey demineralization. *Materials Today: Proceedings.* 2015. **2**(6): 3864.
23. Myronchuk V.G., Dzyazko Yu.S., Zmievskii Yu.G., Ukrainets A.I. Organic-inorganic membranes for filtration of corn distillery. *Acta Periodica Technologica*. 2016. **47**: 153.

24. Dzyazko Y.S., Rozhdestvenska L.M., Vasilyuk S.L., Kudelko K.O., Belyakov V.N. Composite membranes containing nanoparticles of inorganic ion exchangers for electrodialytic desalination of glycerol. *Nanoscale Res. Lett.* 2017. **12**(1): 1.
25. Liu S., Tian J., Zhang W. Fabrication and application of nanoporous anodic aluminum oxide: a review. *Nanotechnology*. 2021. **32**(22): 222001.
26. Poinern G.E.J., Ali N., Fawcett D. Progress in nano-engineered anodic aluminum oxide membrane development. *Materials (Basel).* 2011. **4**(3): 487.
27. Lee W., Park S.-J. Porous anodic aluminum oxide: anodization and templated synthesis of functional nanostructures. *Chem. Rev*. 2014. **114**(15): 7487.
28. Xia Z., Riester L., Sheldon B.W., Curtin W.A., Liang J., Yin A., Xu J.M. Mechanical properties of highly ordered nanoporous anodic alumina membranes. *Rev. Adv. Mater. Sci*. 2004. **6**(2): 131.
29. Platschek B., Keilbach A., Bein T. Mesoporous structures confined in anodic alumina membranes. *Adv. Mater*. 2011. **23**(21): 2395.
30. Yuan J.H., He F.Y., Sun D.C., Xia X.H. A Simple method for preparation of through-hole porous anodic alumina membrane. chemistry of materials. *Chem. Mater*. 2004. **16**(10): 1841.
31. Yuan J.H., Chen W., Hui R.J., Hu Y.L., Xia X.H. Mechanism of one-step voltage pulse detachment of porous anodic alumina membranes. *Electrochim. Acta.* 2006. **51**(22): 4589.
32. Mardilovich P.P., Govyadinov A.N., Mukhurov N.I., Rzhevskii A.M., Paterson R. New and modified anodic alumina membranes Part I. Thermotreatment of anodic alumina membranes. *J. Membr. Sci*. 1995. **98**(1–2): 131.
33. Patel Y., Palevičius A., Naginevičius V., Liaudanskaite J., Janušas G. Aluminum oxide membrane as a functional element for filtering bioparticles in micro hydraulic devices. In: *Frontiers in Ultrafast Optics: Biomedical, Scientific, and Industrial Applications XX.* Proc. SPIE11270. 2020. P. 1127004.
34. Osmanbeyoglu H., Hurb Tae Bong, Kim Hong Koo. Thin alumina nanoporous membranes for similar size biomolecule separation. *J. Membr. Sci*. 2009. **343**: 1.
35. Attaluri A.C., Huang Z., Belwalkar A., Geertruyden W.V., Gao D., Misiolek W. Evaluation of nano-porous alumina membranes for hemodialysis application. *ASAIO J*. 2009. **55**(3): 217.
36. Sharma A. Ph.D (Chem.) Thesis. (London, 2018).
37. Joung C.-K., Kim H.-N., Lim M.-C., Jeon T.-J., Kim H.-Y., Kim Y.-R. A nanoporous membrane-based impedimetric immunosensor for label-free detection of pathogenic bacteria in whole milk. *Biosens. Bioelectron*. 2013. **44**: 10.
38. Su T., He L., Mo R., Zhou C., Wang Z., Wan Y., Li C. A non-enzymatic uric acid sensor utilizing ion channels in the barrier layer of a porous anodic alumina membrane. *Electrochem. Commun*. 2018. **96**: 113.
39. Vandekerkhove A., Negahdar L., Glas D. Synthesis and characterization of Ru-loaded anodized aluminum oxide for hydrogenation catalysis. *ChemistryOpen*. 2019. **8**(4): 532.
40. Liu C., Gillette EI., Chen X., Pearse A.J., Kozen A.C., Schroeder M.A., Gregorczyk K.E., Lee S.B., Rubloff G.W. An all-in-one nanopore battery array. *Nat. Nanotechnol*. 2014. **9**: 1031.
41. Ahn Y., Park J., Shin D., Cho S., Park S.Y., Kim H., Kim Y.S. Enhanced electrochemical capabilities of lithium ion batteries by structurally ideal AAO separator. *J. Mater. Chem. A*. 2015. **3**(20): 10715.
42. Shi W., Shena Y., Gea D., Xue M., Cao H., Huanga S., Wangc J., Zhangc G., Zhangc F. Functionalized anodic aluminum oxide (AAO) membranes for affinity protein separation. *J. Membr. Sci.* 2008. **325**(2): 801.
43. Hou P., Liu C., Shi C., Cheng, H. Carbon nanotubes prepared by anodic aluminum oxide template method. *Chin. Sci. Bull.* 2011. **57**(2–3): 187.
44. Sui Y., Cui B., Guardián R., Acosta D., Martínez L., Perez R. Growth of carbon nanotubes and nanofibres in porous anodic alumina film. *Carbon.* 2002. **40**(7): 1011.
45. Yang S.M., Chen K.H., Yang Y.F. Synthesis of polyaniline nanotubes in the channels of anodic alumina membrane. *Synthetic Metals.* 2005. **152**(1–3): 65.
46. Wang D., Zhang L., Lee W., Knez M., Liu L. Novel three-dimensional nanoporous alumina as a template for hierarchical $TiO_2$ nanotube arrays. *Small*. 2013. **9**(7): 1025.
47. Rozhdestvenka L.M., Kudelko K.O., Ogenko V.M., Menglei Ch. Membrane materials based on porous anodic aluminium oxide *Ukr. Chem. J.* 2020. **86**(12): 67.
48. Kudelko K., Rozhdestvenskaya L., Ogenko V., Chmilenko V. Formation and characterisation of porous anodized aluminum oxide, synthesized electrochemically in the presence of graphene oxide. *Appl. Nanosci.* 2022. **12**: 1967.
49. Li Z., Fan G., Tan Z., Guo Q., Xiong D., Su Y., Zhang D. Uniform dispersion of graphene oxide in aluminum powder by direct electrostatic adsorption for fabrication of graphene/aluminum composites. *Nanotechnol.* 2014. **25**(32): 325601.
50. Ding R., Li W., Wang X., Gui T., Li B., Han P., Song L. A brief review of corrosion protective films and coatings based on graphene and graphene oxide. *J. Alloys Compd*. 2018. **764**: 1039.

51. Ivaništšev V., Fedorov M.V., Lynden-Bell R.M. Screening of Ion–Graphene Electrode Interactions by Ionic Liquids: The Effects of Liquid Structure. *J. Phys. Chem. C.* 2014. **118**(11): 5841.
52. Kong N., Liu J., Kong Q., Wang R., Barrow C.J., Yang W. Graphene modified gold electrode via π–π stacking interaction for analysis of $Cu^{2+}$ and $Pb^{2+}$. *Sens. Actuators, B*. 2013. **178**: 426.
53. Yang Y., Asiri A.M., Tang Z., Du D., Lin Y. Graphene based materials for biomedical applications. *Mater. Today*. 2013. **16**(10): 365.
54. Perlova O.V., Ivanova I.S., Dzyazko Y.S., Danilov M.O., Rusetskii I.A., Kolbasov G.Ya. Sorption of U(VI) compounds on inorganic composites containing partially unzipped multiwalled carbon nanotubes. *Him. Fiz. Tehnol. Poverhni.* 2021. **12**(1): 18.
55. Perlova O.V., Dzyazko Yu. S., Palchik A.V., Ivanova I.S., Perlova N.O., Danilov M.O., Rusetskii I.A., Kolbasov G.Ya., Dzyazko A.G. Composites based on zirconium dioxide and zirconium hydrophosphate containing graphene-like additions for removal of U(VI) compounds from water. *J. Appl. Nanosci.* 2020. **10**: 4591.
56. Luo X., Wang C., Wang L., Deng F., Luo S., Tu X., Au C. Nanocomposites of graphene oxide-hydrated zirconium oxide for simultaneous removal of As(III) and As(V) from water. *Chem. Eng. J*. 2013. **220**: 98.
57. Rozhdestvenska L., Kudelko K., Ogenko V., Palchik O., Plisko T., Bildyukevich A, Zakharov V., Zmievskii Y., Vishnevskii O. Filtration membranes containing nanoparticles of hydrated zirconium oxide–graphene oxide. In: *Springer Proceedings in Physics: Nanomaterials and Nanocomposites, Nanostructure Surfaces, and Their Applications*. 2020. **246**: 757.
58. Wang X., Zhao Y., Tian E., Li J., Ren Y. Graphene oxide-based polymeric membranes for water treatment. *Adv. Mater. Interfaces.* 2018. **5**(15): 1701427.
59. Ng L.Y., Chua H.S., Ng C.Y. Incorporation of graphene oxide-based nanocomposite in the polymeric membrane for water and wastewater treatment: A review on recent development. *J. Environ. Chem. Eng*. 2021. **9**(5): 105994.
60. Ogenko V., Orysyk S., Kharkova L., Yanko O., Chen D. Synthesis and spectral characteristics of Cu(II), Ni(II) and Fe(III) nanosized com-plexes on the surface of carbon quantum dot. *Ukr. Chem. J*. 2021. **87**(9): 3.
61. Sulka G.D. *Highly ordered anodic porous alumina formation by self-organized anodizing*. (WILEY-VCH, 2008).
62. Goa J. A micro biuret method for protein d determination of total protein in cerebrospinal fluid. *Scand. J. Clin. Lab. Invest.* 1953. **5**(3): 218.
63. Dzyazko Yu., Ogenko V. *Polysaccharides: An efficient tool for fabrication of carbon nanomaterials. in: polysaccharides: properties and applications*. (Wiley-Scrinever, Hoboken, Beverly, 2021). P. 337.
64. Nielsch K., Choi J., Schwirn K., Wehrspohn R.B., Gösele U. Self-ordering regimes of porous alumina: the 10 porosity rule. *Nano Lett*. 2002. **2**(7): 677.
65. Barathi M., Krishna Kumar A.S., Kumar C.U., Rajesh N. Graphene oxide–aluminium oxyhydroxide interaction and its application for the effective adsorption of fluoride. *RSC Adv*. 2014. **4**(96): 53711.
66. Che Y., Sun Z., Zhan R., Wang S., Zhou S., Huang J. Effects of graphene oxide sheets-zirconia spheres nanohybrids on mechanical, thermal and tribological performances of epoxy composites. *Ceram. Int*. 2018. **44**(15): 18067.
67. Bogoyavlensky A.F. *The mechanism of formation of anodic oxide film on aluminum*. (Moscow: Mashinostroenie, 1964). [in Russian].
68. Garsia-Vergara S.J., Skeldon P., Thompson G.E., Habazaki H. Formation of porous anodic alumina in alkaline borate electrolyte. *Thin Solid Films*. 2007. **515**(3): 5418.
69. Lee W., Ji R., Gösele U., Nielsch K. Fast fabrication of long-range ordered porous alumina membranes by hard anodization. *Nat. Mater*. 2006. **5**: 741.
70. Dzyazko Yu.S., Rozhdestvenskaya L.M., Vasilyuk S.L., Belyakov V.N., Kabay N., Yuksel M., Arar O., Yuksel U. Electro-deionization of Cr (VI)-containing solution. Part I: chromium transport through granulated inorganic ion-exchanger. *Chem. Eng. Commun*. 2008. **196**(1–2): 3.


*Received 12.09.2022, accepted 05.06.2023*